Engineered Science
DOI: https://dx.doi.org/10.30919/es1601

Assessment of the Hazard Zones for Certain Fire Scenarios Using a Numerical Experiment Design

Alphonse Tchoukouabe,[1, 3,*] Zacharie Merlin Ayissi,[1, 2, 3] Batambock Samuel [2] and Ruben Mouangue[1, 2]

Abstract

This study aims to develop simplified mathematical models for the evaluation of hazard zones belonging to scenarios such as flash fire, jet fire, and BLEVE (Boiling Liquid Expanding Vapour Explosion). The combinations of parameters at two levels obtained through an experimental design were simulated using the Areal Locations of Hazardous Atmospheres (ALOHA) software. Statistical analysis using determination coefficient (R^2), Akaike information (AIC) and root mean square error (RMSE) revealed that the quadratic model was the best. ANOVA helped assess the significant parameters, and the response surface methodology highlighted the interaction of these parameters. For a flash fire, the coupling of wind speed and discharge hole diameter was the most significant, resulting in a distance of 391 m and 911 m for the red and yellow danger zones. In the case of a jet fire, air temperature and discharge hole diameter were the most significant, generating the impact distances of 47 m, 68 m and 106 m for the red, orange and yellow hazard zones, respectively. Finally, in the case of a BLEVE scenario, the tank filling rate and air temperature generate the significant distances of 445 m, 629 m and 981 m for the red, orange and yellow hazard zones. These results could help to improve the management of future incidents.

Keywords: Modeling; Hazard zone; Parameters; Experimental design.

Received: 12 November 2024; Revised: 19 March 2025; Accepted: 15 May 2025.
Article type: Research article.

1. Introduction

Hydrocarbons are of great importance for meeting consumers' energy needs. Their distribution requires transportation methods, which constitute a central issue in oil supply, including at the national level. It is necessary to find safe delivery routes while optimizing costs.[1] Different transportation methods are possible, with rail being the most commonly used.[2] During transportation, harmful incidents can occur. Such an event also involves both direct and indirect harmful effects on the population and the environment, particularly when transporting hazardous or polluting substances.[3] The transport of crude oil by rail has increased considerably in recent years.[4] Transporting toxic, flammable and explosive substances by rail involves major risks because of their volume.[5] A hydrocarbon release during an incident can lead to several fire scenarios. A devastating accident due to a crude oil vapor explosion resulted in 62 deaths and 136 injuries on November 22, 2013, in Qingdao, China.[6] On February 3rd, 2023, a Norfolk Southern train traveling through East Palestine, Ohio derailed, releasing toxic chemicals into the nearby soil, waterways, and air. This prompted mass evacuations of East Palestine's residents.[7] Fire scenarios generate hazard zones, so the assessment of hazard zones generated by fire scenarios is a very useful area of research for safety and accident control.

During the last few decades, a number of research studies have focused on several methods for assessing the hazard zones generated by fire scenarios, including computational fluid dynamics (CFD) simulation, semi-empirical modeling and dispersion models.[8] For CFD codes, Sun *et al*.,[9] use the CFD model in Ansys Fluent software for hazard zone assessment. Thus the study by Palacio *et al*.[10] provides a compilation and comprehensive discussion of the most important aspects of CFD modeling for simulating

[1] *Laboratory of Energy Mecatronic,Energiatronic and sustainable Mobility LMEMD, University of Douala, Douala, P.O. Box 2701, Cameroon*
[2] *National Higher Polytechnic School, University of Douala, Douala, P.O. Box 2701, Cameroon*
[3] *Department of Automotive Engineering and Mechatronics, ENSPD, University of Douala, Douala, P.O. Box 2701, Cameroon*
* *E-mail:* Tchoukouabele3m@gmail.com (A. Tchoukouabe)

hydrocarbon fires in the open environment. The FDS software is the most widely used code. Semi-empirical models include the Solid Flame Model (SFM) and the Point Source Model (PSM).[11,12] With regard to other methods Boot through their study models thermal radiation from pool and jet fires,[13] discretizes the flame in EFFECT software and evaluates the danger zone. According to the works of Misic *et al*.,[14] two simulation tools where used, namely the Areal Locations Of Hazardous Atmospheres (ALOHA) and: Process Hazard Analysis Software Tool (PHAST) to evaluate the distance of thermal radiation for a pool fire. Similarly, Bernatik *et al*.[15] used simulation tools such as ALOHA, EFFECTS GIS (software of the Dutch company TNO) and TerEX (software of the Czech company T-SOFT) to evaluate the impact distance lading to the dispersion of more chemical product.

Previous studies reveal that several methods are used to assess the danger zones generated by fire scenarios. The use of commercial codes and considerable computer resources are the most popular. Although the use of free code such as the Areal Locations of Hazardous Atmospheres (ALOHA) program has proved invaluable in improving the accuracy and reliability of accident consequence predictions.[16] Despite the advantages of the ALOHA software. Simplified models for predicting hazard zones have been the subject of some work, following the example of Alfonse *et al*. (2022),[17] who proposed simplified mathematical models for evaluating hazard zones. The method consisted of combining a numerical design of experiment with numerical simulation using the ALOHA programme. Their study was limited to the evaluation of danger zones for a toxic gas dispersion using five parameters such as wind speed, ambient temperature, humidity level, diameter of the discharge hole and height of the discharge hole on the tank. Similarly Didem *et al.* used the same method,[18] integrating a Box-Behnken design of experiment, to propose mathematical models for evaluating hazard distances for scenarios such as VCE (Vapour Cloud Explosion), Jet and BLEVE (Boiling Liquid Expanding Vapour Explosion) using three parameters such as wind speed, ambient temperature and tank filling rate. However, the method used by Alfonse *et al*.[17] and Didem *et al*.[18] was limited to using a few variables in their prediction models when applied to certain fire scenarios, which could reduce its effectiveness when used. The innovation in this study consists of integrating more parameters such as wind speed, ambient temperature, humidity level, tank filling rate, discharge hole diameter and discharge hole position height into the prediction model development method. For fire scenarios such as flash fire, jet and BLEVE, and to have more information on the interactions that may exist between the parameters. However, the method used by Alfonse *et al*.[17] and Didem *et al*.[18] was limited to using a few variables in their prediction models when applied to certain fire scenarios, which could reduce its effectiveness when used. The innovation in this study consists of integrating more parameters such as wind speed, ambient temperature, humidity level, tank filling rate, discharge hole diameter and discharge hole position height into the prediction model development method. For fire scenarios such as flash fire, jet and BLEVE, and to have more information on the interactions that may exist between the parameters.

In this study, the main objective is to propose simplified mathematical models for assessing hazard zones for scenarios such as flash fire, jet and BLEVE. Firstly, the ALOHA software is used to simulate the different combinations obtained from a design of experiments for the different fire scenarios. Then, the responses obtained are analyzed to elaborate the different models, and finally, the interaction of the significant parameters of each hazard zone belonging to fire scenarios is studied using the surface response method. The results of this study can be used as a decision-making aid for emergency response plans.

2. Materials and methods

2.1 Theoretical model of fire scenarios

This section describes the different fire scenarios studied and their consequences.

2.1.1 Flash fire

It is the leakage of a product that creates a flammable vapor cloud, which mixes with the air and may ignite in the presence of a heat source. The flammable zone is limited by two values related to the Lower Explosive Limit (LEL). This is the lowest concentration of a particular gas that can be flammable or combustible. Gases below the LEL will not feed or sustain an explosion, given that these concentrations are considered too lean. The Upper Explosive Limit (UEL) is the highest concentration of a gas in the air capable of producing a flash fire when it encounters an ignition source. Concentrations above the UEL will not feed or sustain an explosion, given that these concentrations are considered too rich.[19] Fig. 1 graphically shows the manifestation of hazard zones for a flash fire scenario. The red zone indicates the upper explosive limit, which must have a maximum concentration of 17,000 ppm, and the yellow zone indicates the lower explosive limit, accounting for a minimum concentration of 2,800 ppm.

2.1.2 Jet fires

A jet fire occurs when a pressurized hydrocarbon fluid flows through an orifice and, in the presence of a heat source, ignites

to form a jet flame. Jet fires are associated with very high heat fluxes, and if they come into contact with equipment, they can cause catastrophic failure in a very short time.[20]

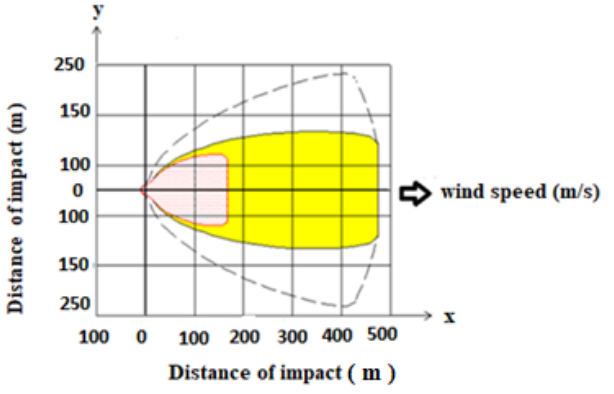

Fig. 1: Ignition zone for a flash fire scenario.

2.1.3 BLEVE

A BLEVE (Boiling Liquid Expanding Vapor Explosion) is the explosion of a substance that has reached its critical temperature. It is generally followed by a fireball and intense thermal radiation.[21] The fireball goes through three phases (growth, combustion, and extinction), rises to a certain height in a spherical shape, and then takes on the form of a mushroom cloud.[22] The thermal energy is released in a short amount of time. Fig. 2 shows the zones generated by thermal radiation for a jet fire and a BLEVE. The probable fatality zone is the red zone, second-degree burn zone is the orange zone, and the body pain zone is the yellow zone. The boundary conditions defining the hazard zones for each scenario are shown in Table 1.

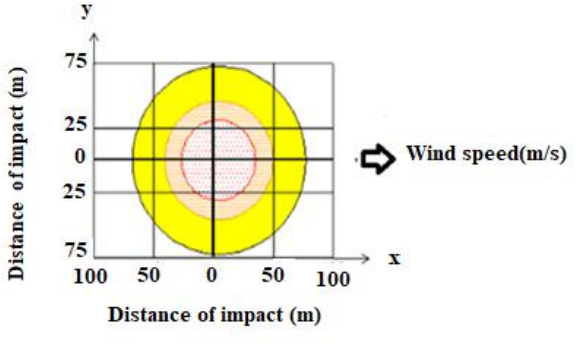

Fig. 2: Thermal radiation zone for a Jet and BLEVE fire.

2.1.4 ALOHA

ALOHA is based on conceptual and mathematical models designed to simulate dispersion and capable of estimating hazard zones caused by the release of hazardous chemicals, toxic vapor clouds, fires, and explosions. ALOHA uses a graphical interface for data entry and results display. Exposures to toxic chemical vapors, overpressure, thermal radiation, or areas with flammable gases are graphically represented and accompanied by a textual summary.[16]

Table 1: Conditions limiting hazard zones.[23]

Consequence	Red	Orange	yellow
Flash fire (the vapour cloud ignites)	60% LEL (17000ppm)		10%LEL (2800ppm)
Thermal radiation (BLEVE - JET fire)	Potential for death for 60s (10.0 kw/m^2)	2nd degree burn for 60s (5.0 KW/m^2)	Slight burn for 60s (2.0 KW/m^2)

2.2 Data used

Table 2 shows the values of each variable applied in the simulations. The soil roughness used was urban/forest. The dimensional characteristics of the tank used are shown in Fig. 3.

2.2.1 Atmospheric parameters

The atmospheric parameters used are those derived from the atmospheric conditions in Cameroon: wind speed (A), ambient temperature (B) and humidity (C).

2.2.2 Release parameters

Transport accidents can be collisions or derailments, which can result to several types of release: instantaneous release (less than one minute); critical release (catastrophic rupture of 300 mm release hole) and semi-continuous release for a 50 mm diameter.[24] For this study, we consider a semi-continuous discharge with a discharge hole diameter (E) varying from 15 mm to 50 mm and the discharge hole position (F) either at the bottom of the tank or in the middle of the tank, 2 m from the bottom .

2.2.3 Filling rate for wagon tanks

According to regulations, the fill rate must never exceed 95%. In this study, the filling rate (D) varied from 50% to 95%.[25] The selection of the various data in the table is based on the study carried out by Alphonse *et al*.,[26] repetorizing for each fire scenario the parameters that influence them

2.3 Experimental design and statistical analysis

2.3.1 Modelling using the Box Behnken design (BBD) of experiment

The Box-Behnken experimental design, developed by Box and Behnken in 1980, is one of the most commonly used designs, along with the Central Composite Design (CCD), and

is used to develop second-order response surface models. This type of design is based on the construction of balanced incomplete block designs and requires at least three levels for each factor.[27,28] BBD is often considered a relatively efficient and ideal alternative to CCD,[29,30] hence the motivation for its use in this study. Each simulated scenario has four factors at two levels 24. The coding of the factors for each fire scenario can be found in Table 2. The design-expert program was used to establish the experimental design, and the combinations are simulated using the ALOHA software, which evaluates the impact distance for each combination of the experimental design according to each scenario. Tables S1-S3 of the experimental designs for the different scenarios.

2.3.2 Statistical analysis

Several tools are used to select and analyse the mathematical model.

2.3.2.1 Data analysis

Analysis consists in checking the shape and types of distribution of the data set. Two tools are used: skewness, which calculates the symmetry of the data set, and kurtosis, which is the kurtosis coefficient representing the distance at which the data moves away from the mean, or the distance at which it moves towards it.[31] A negative skewness coefficient indicates that most of the data lie to the right of the mean and that the tail to the left is longer, while a positive skewness coefficient indicates that most of the data lie to the left of the mean and that the tail to the right is longer,[32] and a positive kurtosis coefficient indicates that the distribution is sharper than the normal distribution. On the other hand, a negative kurtosis coefficient indicates that the distribution is flatter than the normal distribution.[33]

2.3.2.2 Model selection

Three tools were used to select the model. The coefficient of determination (R^2), according to Eq. (1), refers to the proportion of the variance of the response variable explained by an adjusted model, compared with simply taking into account the mean of the response. [34] The Akaike information criterion (AIC) Eq. (2) is a measure of the quality of a statistical model, and the root mean square error (RMSE). Eq. (3) measures the average difference between a statistical model's predicted values and the actual values. Selection criteria: (Worst value = −∞; best value = +1).

$$R^2 = \frac{\sum_{i=1}^{m}(X_i - Y_i)^2}{\sum_{i=1}^{m}(\bar{Y} - Y_i)^2} \quad (1)$$

where X_i is the predicted ith value, and the Y_i element is the actual ith value.

$$AIC_i = 2k_i - 2\log(l_i) \quad (2)$$

where k is the number of model parameters to be estimated and L is the maximum likelihood function of the model.

$$RMSE = \sqrt{\frac{1}{m}\sum_{i=1}^{m}(X_i - Y_i)^2} \quad (3)$$

where X_i is the predicted ith value, and the Y_i element is the actual ith value

2.3.2.3 Model analysis

ANOVA was used to evaluate and analyze the effects of the different variables on responses within a 95% confidence interval.[35] Eq. (4) is used to calculate the F-value, which is the ratio between the mean squares of the treatment ($MSTr$) and the mean squares of the error MSE (error variance), this tool is used to evaluate the significance of a parameter.[36]

$$F_o = \frac{\frac{SST_r}{a-1}}{\frac{SSE}{a(n-1)}} \quad (4)$$

where $SSTr$ is the sum of squares of the treatment, SSE is the sum of squares of the error, (a - 1) represents the degrees of freedom of the treatment, (n - 1) represents the degrees of freedom of the error, a is the number of treatments (number of samples), n is the number of observations for a particular treatment.

2.3.2.4 Uncertainty analysis and model validation

Two tools were used to assess the limits and uncertainties of the chosen model. The reduced Chi-Sqr represents the error between the fitted values and the actual values.[37] As the reduced Chi-Sqr approaches 0, the error of the simulated value becomes smaller and the confidence interval (CI) indicates whether the estimate is accurate or only a very rough estimate.[38] A narrower CI indicates a more accurate estimate, while a wider CI indicates a less accurate estimate.[39] Through 3D graphical representations, called response surfaces, the interaction of each model's significant variables is described. The flowchart in Fig. 4 shows the various stages involved in achieving the desired results. At the end, each scenario presents a mathematical model for calculating the impact zones.

3. Results and discussion

3.1 Analysis of response

The maximum and minimum distances and distribution shape indicators for each scenario are summarized in Table 3 for

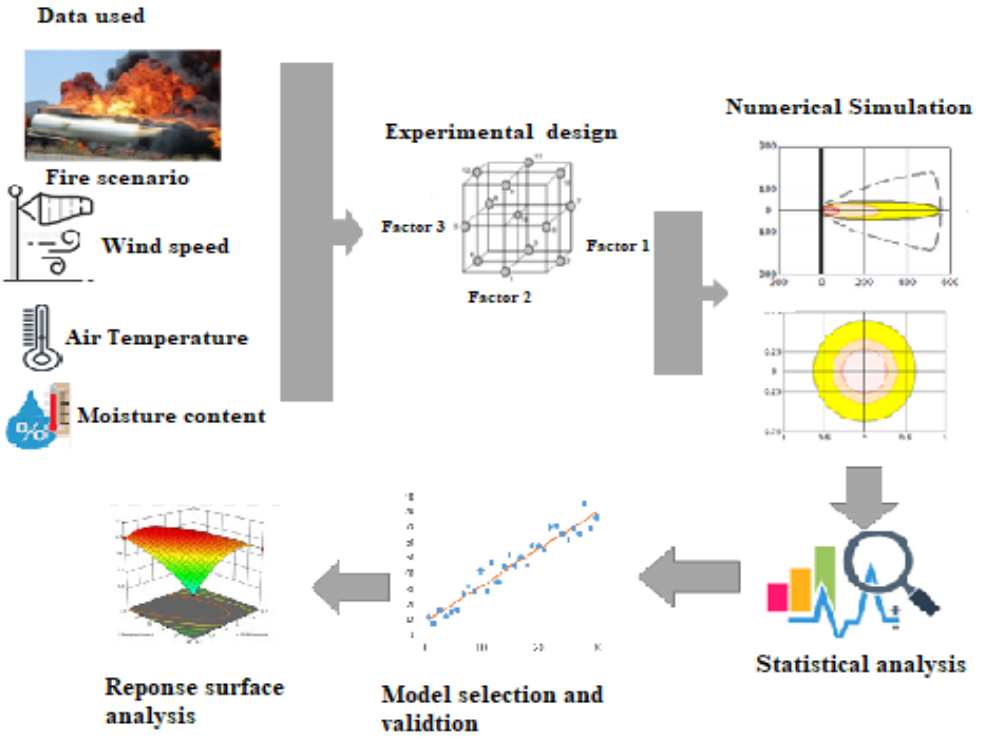

Fig. 4: Study organization chart.

Table 3: Summary of maximum and minimum distances for fire scenarios.

Scenario	Distances								
	Hazard zones	Units	obs	Min	Max	Mean	St dev	Skewness	Kurtosis
Flash fire	red	m	30.00	68	391	186.17	78.85	0.451	0.297
	yellow	m	30.00	174	911	452.27	181.19	0.391	0.246
Jet	red	m	30.00	14	47	30.47	9.90	-0.088	-0.361
	orange	m	30.00	20	68	43.77	14.46	-0.033	-0.352
	yellow	m	30.00	32	106	68.53	22.72	-0.034	-0.361
BLEVE	red	Km	30.00	340	445	393.13	26.30	-0.149	-0.404
	yellow	Km	30.00	480	629	555.30	37.22	-0.164	-0.395
	red	Km	30.00	748	981	864.87	57.97	-0.146	-0.401

each hazard zone and fire scenario. For the flash fire scenario, the minimum distances for the red and yellow hazard zones are respectively 68 m; 174 m; when the combination is wind speed (1.9 m/s); air temperature (24.5 °C); discharge hole diameter (1.5 cm) and discharge hole height position (2 m). The maximum distance varies from 391 m to 911 m belonging respectively to the red and yellow zones when the combination is made up of wind speed at 1.3 m/s, air temperature at 24.5 °C, discharge hole diameter at 5 cm positioned 1 m from the bottom of the tank. It can be seen from Fig. 5a that the danger zones increase when the diameter of the discharge hole varies from 1.5 cm to 5 cm, and fall from Fig. 5b when the wind speed varies from 1.9 m/s to 1.3m/s, which could indicate that hole diameter and wind speed are parameters to be taken into account in safety measures for a toxic gas dispersion scenario.

As a result, for a jet fire scenario, the minimum distance for the red, orange and yellow danger zones are respectively 14 m; 20 m; 32 m when the combination is made up of wind speed (1.9 m/s); air temperature (14 °C); humidity level (70) and discharge hole diameter (1.5 cm). The maximum distance in the different zones (red, orange and yellow) are respectively 47 m, 68 m and 106 m when the combination is made up of wind speed at (1.9 m/s), air temperature at (35 °C), humidity level (70) and reject hole diameter at 5 cm. According to Figs. 5c and 5d, the danger zones increase as the diameter of the discharge hole varies from 1.5 cm to 5 cm and as the temperature varies from 35 °C to 14 °C, which could indicate that hole diameter and air temperature are parameters to be considered in safety measures for a jet fire scenario.

Finally, for a BLEVE scenario, the minimum distance for the red, orange and yellow danger zones are respectively 340 m; 480 m; 748 m when the combination is made up of wind speed (1.9 m/s); air temperature (35 °C); humidity level (70%) and tank filling level (50%). the maximum distance in the

different zones (red, orange and yellow) are respectively 445 m, 629 m and 981 m when the combination is made up of wind speed (1.9 m/s), air temperature (14 °C), humidity level (70) and tank filling level (95%). From Fig. 5e, we can see that the danger zones increase with the tank filling rate from 50 to 95%, and when the temperature varies from 35 °C to 14 °C, as shown in Fig. 5f, the impact zone drops. Filling rate and air temperature are parameters that vary the impact zones for a BLEVE scenario.

Looking at the distribution shape indicators for each scenario. We can see that for a flash fire the skewness is greater than zero, *i.e.*, 0.451 and 0.391, and the kurtosis greater than zero, *i.e.*, 0.297 and 0.246 respectively for the red and yellow zones. For the Jet and BLEVE fire scenarios, Skewness and kurtosis are below zero in all hazard zones associated with each fire scenario. Following the Skerwness and Kurtosis values for the flash fire scenario, the distribution is asymmetrical, with a sharper shape spread to the right of the mean. The Jet and BLEVE fire scenarios show a more asymmetrical distribution, with a flatter shape spread to the left of the mean. According to Demir *et al.*[32] the acceptable interval for asymmetry and kurtosis coefficients is ±1, which is in line with our results.

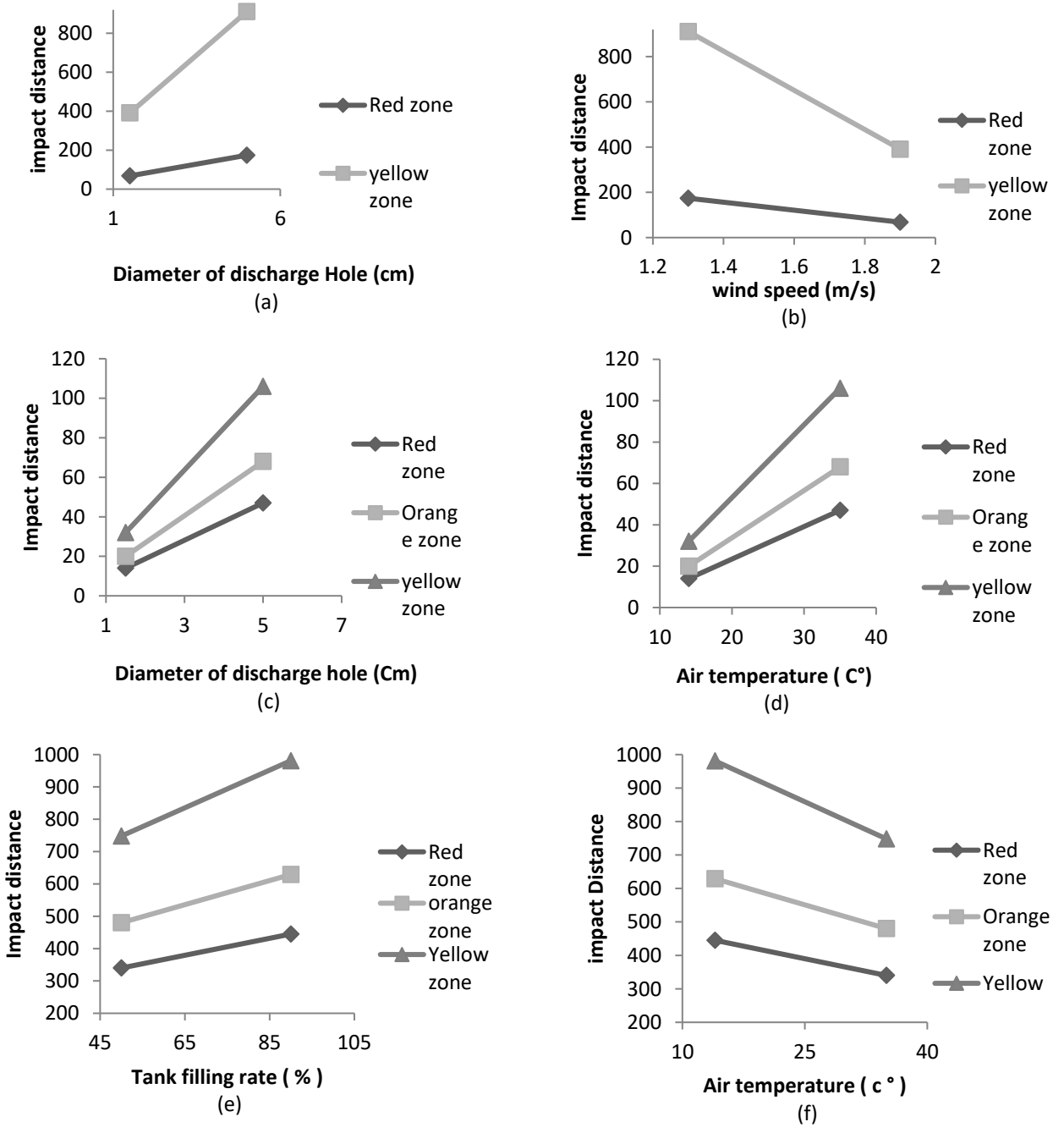

Fig. 5: Influence of certain parameters on hazard distance: flash fire diameter of discharge hole (a), wind speed (b); jet fire scenario diameter of discharge hole (c), Air temperature (d); BLEVE Tank filling rate (e) and air temperature (f).

3.2 Choice of models for the different scenario

The different statistical models (linear, inter-factor action, quadratic and cubic) are presented in Tables 4-6. The selection criterion is based on the highest R^2 correlation, the model with the lowest AIC and the lowest mean squared error.[40]

The model summaries for the flash fire scenario are presented in Table 4, showing a preference for quadratic models with a high R^2 correlation to other models. For an R^2 predicted in the red and yellow zones we have 0.9683 and 0.9652 respectively. These correlations of the different zones are in reasonable agreement with the adjusted R^2 of these zones, *i.e.* 0.9894 (red) and 0.9883 (yellow), with a difference of less than 0.2 for the red and yellow zones. The quadratic model has the lowest AIC value, 254.41 and 307.10 respectively for the red and yellow zones, and the lowest mean squared error.

Table 5 presents the models for the jet fire scenario. It can be seen that the quadratic model has high R^2 compared with the other models. For R^2 predicted in the red, orange and yellow zones we have 0.9993, 0.9996 and 0.9999 respectively. These correlations for the different zones are in reasonable agreement with the adjusted R^2 for these zones, *i.e.*, 0.9981 (red), 0.9989 (orange) and 0.9998 (yellow), with a difference of 0.00123, 0.0068 and 0.0001 respectively for the red, orange and yellow zones. The quadratic model has the lowest AIC values of 44.78, 42.26 and 14.42 respectively for the red, orange and yellow zones, and the lowest mean square error.

In the case of BLEVE, Table 6 shows that the quadratic model has the highest R^2 compared with the other model. For R^2 predicted in the red, orange and yellow zones, we have 0.9993, 0.9996 and 0.9999 respectively. These correlations of the different zones are in reasonable agreement with the adjusted R^2 of these zones, *i.e.*, 0.9998 (red), 0.9999 (orange) and 0.9999 (yellow), with a difference of 0.00123, 0.0068 and 0.0001 respectively for the red, orange and yellow zones. The predicted R^2 is in reasonable agreement with the adjusted R^2, *i.e.*, the difference is less than 0.2. The quadratic model has the lowest AIC value, 73.86, 79.50 and 97.13 respectively for the red, orange and yellow zones, and the lowest mean square error.

Table 4: Summary of flash scenario models.

Scenario			Models			
	IMPACT	TOOLS	LINEAR	2FI	QUADRATIC	CUBIC
Flash fire: ignition zone	Red	Adjusted R^2	0.941	0.949	0.989	0.999
		Predicted R^2	0.921	0.891	0.968	0.993
		AIC	269.02	280.78	254.41	273.88
		Root-MSE (SD)	17.54	14.39	5.93	0.52
	Yellow	Adjusted R^2	0.943	0.950	0.988	0.999
		Predicted R^2	0.924	0.894	0.965	0.990
		AIC	317.85	329.80	307.10	338.02
		Root-MSE (SD)	39.64	32.61	14,28	1,51
					Suggested	Aliased

Table 5: Summary of Jet fire models.

Scenario			Models			
	IMPACT	TOOLS	LINEAR	2FI	QUADRATIC	CUBIC
Jet fire: area of thermal radiation	Red	Adjusted R^2	0.997		0.999	0.999
		Predicted R^2	0.997	0.996	0.998	0.995
		AIC	45.63	59.88	44.78	138.5
		Root-MSE (SD)	0.434	0.368	0.180	0.054
	Orange	Adjusted R^2	0.999	0.999	0.999	0.999
		Predicted R^2	0.998	0.998	0.998	0.998
		AIC	49.79	43.07	42.26	138.5
		Root-MSE (SD)	0.416	0.274	0.196	0.054
	Yellow	Adjusted R^2	0.999	0.999	0.999	
		Predicted R^2	0.9991	0.9995	0.9998	
		AIC	59.68	52.39	14.43	180.14
		Root-MSE (SD)	0.549	0.325	0.109	0.109
					Suggested	Aliased

Table 6: Summary of BLEVE models.

Scenario			Models			
	IMPACT	TOOLS	LINEAR	2FI	QUADRATIC	CUBIC
BLEVE: thermal radiation zone	Red	Adjusted R^2	0.992	0.991	0.999	0.999
		Predicted R^2	0.990	0.983	0.999	0.995
		AIC	140.2	159.6	73.86	196.9
		Root-MSE (SD)	2.10	1.93	0.293	0.144
	Orange	Adjusted R^2	0.991	0.990	0.999	1.0000
		Predicted R^2	0.989	0.981	0.999	0.999
		AIC	164.80	184.59	79.50	171.51
		Root-MSE (SD)	3.15	2.93	0.322	0.094
	Yellow	Adjusted R^2	0.992	0.991	0.999	1.0000
		Predicted R^2	0.989	0.981	0.999	0.999
		AIC	190.49	209.4	97.13	138.5
		Root-MSE (SD)	4.84	4.44	0.433	0.054
					Suggested	Aliased

Table 7: Adequacy statistics.

Scenarios	Hazard zones	St Dev	Mean	C.V. %	Adeq precision
flash	Red	8.14	186.17	4.37	55.666
	Jaune	19.58	452.27	4.33	52.529
jet	Red	0.24	30.47	0.811	186.87
	Orange	0.268	43.77	0.61	249.96
	Jaune	0.149	68.53	0.217	702.02
BLEVE	Red	0.401	393.13	0.102	374.64
	Orange	0.441	555.3	0.079	482.67
	Jaune	0.5919	864.87	0.006	562.55

For all hazard zones related to the different scenarios, the cubic polynomial was found to be alaisé, and could not be used to fit the final model. All the quadratic models have correlations that are close to 100%, so the estimated regression equation corresponds better to the real data.[41] The difference between R^2 fit and prediction for all the quadratic models are less than 0.02, which could satisfy the requirements of assessing the hazard zones of the different scenarios. The quadratic model has the lowest AIC and the lowest mean square error.[40] The adequacy of the quadratic models of the zones belonging to the different scenarios is analysed in Table 7. It can be seen that the Adeq accuracy is well above 4, which indicates that the models are adequate and that they are navigable.[27] Thanks to these models, it is possible to assess the danger zone generated by the different scenarios. Generally, a standard deviation greater than the mean value produces the variation coefficients greater than 1. In this study, Table 7 shows a very low CV, which indicates very low variability of the parameters around the mean and also gives the best measure of effectiveness.[43,44]

3.3 Model analysis

3.3.1 ANOVA hazard zone model flash fire scenario

The ANOVA applied to the quadratic model for evaluating the danger zone of a flash fire scenario is presented in Table 8. It can be seen that the F-values of the red and yellow zone models are 193.49 and 176.32 respectively. There is only a 0.01% chance that such a high F-value is due to error. P values of less than 0.0500 indicate that the model terms are significant. In this case, wind speed (A), air temperature (B), discharge hole diameter (E), discharge hole position (F), A*E; E*F; A^2; F^2 and A; B; E; F; A*E; B*E; E*F; A^2; F^2 are significant model terms for the red and yellow hazard zones respectively. It can also be seen that the main parameters such as wind speed (A), air temperature (B), discharge hole diameter (E) and hole position (F) are significant for both the red and yellow hazard zones. The interaction between the diameter of the discharge hole and parameters such as wind speed and the position of the discharge hole are significant for the red and yellow zones. It can equally be seen that the diameter of the discharge hole, the interaction between wind speed and the diameter of the discharge hole have a high F value compared with the others.

3.3.2 ANOVA hazard zone model jet fire scenario

Table 9 presents the analysis of variance of the quadratic model for evaluating the hazard distances for a jet fire. Firstly, for the three hazard zones, we observe a high F value of 3320.12, 5995.66 and 48095.79 respectively. There is only a 0.01% chance that such a high F value is due to error. P values of less than 0.0500 indicate that the model terms are significant. The main parameters such as wind speed (A), air temperature (B), moisture content (C) and discharge hole diameter (E) are significant for all three hazard zones (red, orange and yellow). The interaction between hole diameter and air temperature is significant for all three hazard zones. It can be seen that the diameter of the discharge hole has a high F value compared with the other parameters monitored for air temperature, as does the interaction between the diameter of the discharge hole and the ambient temperature.

3.3.3 ANOVA BLEVE scenario hazard zone model

Table 10 presents the results of the ANOVA for the hazard zone assessment models related to a BLEVE scenario. Firstly, for the red, orange and yellow hazard zones, we observe a high F value of 8890.51, 14756.83 and 19890.25 respectively. There is only a 0.01% chance that such a high F-value is due to error. P values of less than 0.0500 indicate that the model terms are significant. The main parameters such as air temperature (B), humidity (C) and tank filling rate (D) are significant for all three hazard zones (red, orange and yellow). The interaction between the tank filling rate and parameters

Table 8: Univariate ANOVA for flash fire hazard zone mode.

source	Sum of Squares	df	Mean Square	F-value	p-value	
Red Zone						
Model	1.793E+05	14	12807.95	193.49	< 0.0001	significant
Wind Speed(A)	19120.08	1	19120.08	288.85	< 0.0001	
Air temperature (B)	2352.00	1	2352.00	35.53	< 0.0001	
Diameter of discharge hole (E)	1.479E+05	1	1.479E+05	2233.60	< 0.0001	
High hole on the tank(F)	1900.08	1	1900.08	28.70	< 0.0001	
A*E	2162.25	1	2162.25	32.67	< 0.0001	
E*F	552.25	1	552.25	8.34	0.0113	
A^2	3293.76	1	3293.76	49.76	< 0.0001	
F^2	1043.05	1	1043.05	15.76	0.0012	
Yellow Zone						
Model	9.463E+05	14	67594.54	176.32	< 0.0001	
Wind Speed (A)	68856.75	1	68856.75	179.62	< 0.0001	
Air temperature (B)	17864.08	1	17864.08	46.60	< 0.0001	
Diameter of discharge hole (E)	8.086E+05	1	8.086E+05	2109.27	< 0.0001	
High hole on the tank(F)	10502.08	1	10502.08	27.40	0.0001	
A*E	10404.00	1	10404.00	27.14	0.0001	significant
B*E	2116.00	1	2116.00	5.52	0.0329	
E*F	2550.25	1	2550.25	6.65	0.0209	
A^2	16157.44	1	16157.44	42.15	< 0.0001	
F^2	5553.44	1	5553.44	14.49	0.0017	

Table 9: ANOVA hazard distance model jet fire scenario.

Source	Sum of Squares	df	Mean Square	F-value	p-value	
Red Zone						
Model	2840.55	14	202.90	3320.12	< 0.0001	significant
Wind Speed (A)	2.08	1	2.08	34.09	< 0.0001	
Air temperature (B)	12.00	1	12.00	196.36	< 0.0001	
Moisture content (C)	0.7500	1	0.7500	12.27	0.0032	
Discharge hole diameter (E)	2821.33	1	2821.33	46167.27	< 0.0001	
B*E	1.0000	1	1.0000	16.36	0.0011	
A^2	0.2976	1	0.2976	4.87	0.0433	

Source	Sum of Squares	df	Mean Square	F-value	p-value	
B^2	0.7619	1	0.7619	12.47	0.0030	
C^2	0.2976	1	0.2976	4.87	0.0433	
E^2	2.33	1	2.33	38.18	< 0.0001	
orange Zone						
Model	6062.28	14	433.02	5995.66	< 0.0001	significant
Wind Speed (A)	3.00	1	3.00	41.54	< 0.0001	
Air temperature (B)	21.33	1	21.33	295.38	< 0.0001	
Moisture content (C)	4.08	1	4.08	56.54	< 0.0001	
Discharge hole diameter (E)	6030.08	1	6030.08	83493.46	< 0.0001	
B*E	1.0000	1	1.0000	13.85	0.0020	
C*E	1.0000	1	1.0000	13.85	0.0020	
E^2	0.7619	1	0.7619	10.55	0.0054	
Yellow Zone						
Model	14963.13	14	1068.80	48095.79	< 0.0001	significant
Wind Speed (A)	0.7500	1	0.7500	33.75	< 0.0001	
Air temperature (B)	36.75	1	36.75	1653.75	< 0.0001	
Moisture content (C)	6.75	1	6.75	303.75	< 0.0001	
Discharge hole diameter (E)	14910.75	1	14910.75	6.710E+05	< 0.0001	
A*B	0.2500	1	0.2500	11.25	0.0043	
A*C	0.2500	1	0.2500	11.25	0.0043	
A*E	0.2500	1	0.2500	11.25	0.0043	
B*C	0.2500	1	0.2500	11.25	0.0043	
B*E	2.25	1	2.25	101.25	< 0.0001	
C*E	2.25	1	2.25	101.25	< 0.0001	
A^2	0.5833	1	0.5833	26.25	0.0001	
B^2	0.5833	1	0.5833	26.25	0.0001	
C^2	0.0119	1	0.0119	0.5357	0.4755	
E^2	2.01	1	2.01	90.54	< 0.0001	

Table 10: ANOVA hazard distance model BLEVE scenario.

Source	Sum of Squares	df	Mean Square	F-value	p-value	
Red Zone						
Model	20053.05	14	1432.36	8890.51	< 0.0001	significant
Air temperature (B)	3168.75	1	3168.75	19668.10	< 0.0001	
Moisture content (C)	408.33	1	408.33	2534.48	< 0.0001	
Tank filling level (D)	16354.08	1	16354.08	1.015E+05	< 0.0001	
B*D	16.00	1	16.00	99.31	< 0.0001	
C*D	2.25	1	2.25	13.97	0.0020	
A^2	0.7619	1	0.7619	4.73	0.0461	
C^2	4.76	1	4.76	29.56	< 0.0001	
D^2	86.01	1	86.01	533.87	< 0.0001	
orange Zone						
Model	40171.38	14	2869.38	14756.83	< 0.0001	significant
Air temperature (B)	6348.00	1	6348.00	32646.86	< 0.0001	
Moisture content (C)	784.08	1	784.08	4032.43	< 0.0001	
Tank filling level (D)	32760.75	1	32760.75	1.685E+05	< 0.0001	
B*D	36.00	1	36.00	185.14	< 0.0001	
C*D	2.25	1	2.25	11.57	0.0039	
C^2	10.71	1	10.71	55.10	< 0.0001	

Source	Sum of Squares	df	Mean Square	F-value	p-value	
D^2	207.43	1	207.43	1066.78	< 0.0001	
Yellow Zone						
Model	97462.22	14	6961.59	19890.25	< 0.0001	significant
Air temperature (B)	16206.75	1	16206.75	46305.00	< 0.0001	
Moisture content (C)	2028.00	1	2028.00	5794.29	< 0.0001	
Tank filling level (D)	78570.08	1	78570.08	2.245E+05	< 0.0001	
B*D	100.00	1	100.00	285.71	< 0.0001	
C*D	6.25	1	6.25	17.86	0.0007	
B^2	4.30	1	4.30	12.28	0.0032	
C^2	25.19	1	25.19	71.97	< 0.0001	
D^2	462.01	1	462.01	1320.03	< 0.0001	

such as air temperature and humidity is significant for all three all three impact zones. We can see that the tank filling rate has a high effect compared with the other parameters, followed by air temperature.

Eqs. (5-12) present the quadratic hazard zone distance regression equations for the different scenarios studied. It is made up of the different significant parameters that allow a better prediction of the hazard zone distances. The quadratic model is shown to be suitable for the different hazard zones studied, depending on the fire scenarios. The equations contain the main parameters, the interactions between the parameters and the squared effect of the parameter. The plus (+) and minus (-) symbolizes the positive or negative effect of the parameters in the equation on the response (hazard zone) and each parameter has a coefficient that expresses the contribution of each parameter in the regression equation.

Eqs. (5) and (6) are used to evaluate the hazard distance for a flash fire scenario. The hole diameter (E) is the main parameter and the combination of wind speed and hole diameter (AE) makes a significant contribution to calculating the hazard distance for a flash fire.

$$Z_{RED\ flash} = 181 - 39.91A + 14B + 111E - 12.58F - 23.25AE - 11.75EF + 21.9A^2 - 12.33F^2 \quad (5)$$

$$Z_{YEL\ flash} = 442 - 75.75A + 38.58B + 259.58E - 29.58F - 51AE + 23BE - 25.25EF + 48.54A^2 - 28.45F^2 \quad (6)$$

where $Z_{RED\ flash}$, $Z_{YEL\ flash}$ are the hazard distances for a flash scenario respectively for the zones in meters; A is the wind speed in m/s; B is the ambient temperature in °C; E is the diameter of the discharge hole in cm. F is the height of the discharge hole on the tank in m.

Eqs. (7) to (9) evaluate the hazard distance for a jet fire scenario in three zones, the main parameter diameter of the discharge hole (E) and the combinations of ambient temperature, hole diameter (B*E) and humidity rate, hole diameter (C*E) have a high contribution in the evaluation of the distances belonging to the hazard zones (red, orange and yellow).

$$Z_{RED\ jet} = 31 + 0.41A + B - 0.25C + 15.33E + 0.5BE - 0.20A^2 - 0.33B^2 - 0.208C^2 - 0.58E^2 \quad (7)$$

$$Z_{ORG\ jet} = 44 + 0.5A + 1.33B - 0.58C + 22.41E + 0.5BE - 0.5CE - 0.33E^2 \quad (8)$$

$$Z_{YEL\ jet} = 69 + 0.25A + 1.75B - 0.75C + 32.25E - 0.25AB - 0.25AC + 0.25AE + 0.25BC + 0.75BE - 0.75CE - 0.29A^2 - 0.29B^2 - 0.541E^2 \quad (9)$$

where $Z_{RED\ jet}$; $Z_{ORG\ jet}$; $Z_{YEL\ jet}$ are the hazard distances in meters associated with a jet fire scenario manifested in three zones (red, orange and yellow); humidity content (C) in %. The variables incorporated in these equations are similar to those in Eqs. (7) to (9).

Regression Eqs. (10) to (12) characterize the assessment of hazard distances for a bleaching scenario. The main parameter (D) tank filling rate and the combination of ambient temperature and tank filling rate have high contributions in the different equations.

$$Z_{RED\ bleve} = 394 - 16.25B - 5.8C + 36.91D - 2BD - 0.75CD + 0.33A^2 + 0.833C^2 - 3.54D^2 \quad (10)$$

$$Z_{ORG\ bleve} = 557 - 23B - 808C + 52.25D - 3BD - 0.75CD + 1.25C2 - 5.5D^2 \quad (11)$$

$$Z_{YEL\ bleve} = 867 - 36.75B - 36.75C + 80.91D - 5BD - 1.25CD + 0.79B^2 + 1.91C^2 - 8.2D^2 \quad (12)$$

where $Z_{RED\ BLEVE}$; $Z_{ORG\ BLEVE}$; $Z_{YEL\ BLEVE}$ are the hazard distances in meters related to a BLEVE scenario manifested in three zones (red, orange and yellow); the filling rate (D) in %. The variables incorporated in these equations are similar to those in Eqs. (10) to (12).

3.3.4 Model validation

The limitations and applicability of the proposed models are analyzed in Table 11. Only the reduced Chi-Sqr values belonging to the quadratic models for the flash fire, Jet fire and BLEVE scenarios show small values compared to the others. As the reduced Chi-Sqr approaches 0, the error of the simulated value becomes smaller.[39] This means that the

model has good predictions. Looking at the confidence interval for each model. By observing the confidence interval of each model. The confidence interval is narrower for quadratic models, indicating greater accuracy of estimation.[45] Although the proposed quadratic models are powerful tools for analyzing and predicting the impact distances of fire scenarios, it is essential to understand their limitations and to use them with caution. These models must be used within the limits well established by the variables studied. Generally speaking, it can be said that the models currently used to assess the risks and consequences of accidents have been developed to suit tasks characterized by much simpler boundary conditions and dispersion characteristics than those applicable to real urban areas. However, these models can be applied to obtain approximate results; the resulting hazard zone distances are then conservative, with many uncertainties in the presence of obstacles (tall buildings).

3.3.5 Analysis of parameter interaction, surface response

In this study the combination of the most significant parameters of the quadratic models are analyzed through the response surface. Figures 6 show the different interactions for each scenario in 3D. Figs. 6a and 6b show the interaction of parameters for a flash fire scenario. Fig. 6a presents the interaction between wind speed and the diameter of the release hole. The impact distance decreases when both the wind speed and the diameter of the fluid release hole increase. The effect of wind speed contributes to reducing the impact. In this condition, wind speed accelerates evaporation.[46] In fact, the gas concentration under the wind direction is diluted as the wind speed plays a diffusion role.[23,47] Under its effect, the chemical vapor disperses in the wind direction, and the gas concentration dilutes, reducing the ignition zone.[48] However, when the diameter of the release hole increases and the wind speed decreases, the diameter of the fluid release hole impacts the ignition zone. Indeed, this increase in the diameter of the release hole in a semi-continuous release condition influences the flow rate of fluid exiting the tank, which increases the amount of evaporated fluid, thus enlarging the ignition zone.[22,23] Fig. 6b shows the interaction between the position of the release hole and the diameter of the release hole on the impact zone. When the position of the hydrocarbon release hole is almost at the bottom of the tank and the hole's diameter is 5 cm, the impact zone increases slightly. However, this increase is reduced if the position of the release hole is closer to the top of the tank. The farther the hole is from the bottom of the tank, the less fluid is released, while a hole positioned toward the bottom promotes the complete flow of fluid from the tank. These findings converge with the results of Xie *et al*.,[49] which state that if the leak hole is located in the middle of the tank instead of at the bottom, the liquid leak will turn into a gas leak. Since the liquid level is below the leak orifice, the hazard zone can be influenced.

Figs. 6c and 6d show the evaluation of hazard zones for a jet fire scenario. The interaction between the release hole diameter and the air temperature is presented in Fig. 6c. A reduction in the hazard distance is observed when the release hole diameter decreases, regardless of the ambient temperature. Air temperature helps limit the leakage rate of the overheated liquid and reach a maximum , which also limits the combustion rate of the mass. Consequently, the maximum thermal radiation decreases with the reduction in the leak diameter, which aligns with the findings of Wang *et al*.[12] Fig. 6d shows the interaction between the release hole diameter and the humidity level. It is observed that the thermal zone distance slightly decreases as the humidity level and fill rate increase. Indeed, according to,[50] the effect of humidity on thermal risk increases when humidity decreases. Moreover, the water vapor present in the air influences heat exchange conditions which could likely explain the reduction in the thermal zone when humidity increases.[51]

The interactions of significant parameters in the radiation zones for a BLEVE scenario are presented in Figs. 6e and 6f. The interaction between ambient temperature and the fill rate of the tank is shown in Fig. 6e. This combination generates a larger radiation zone compared to other interactions. When the

Table 11: Analysis of model error and uncertainty.

		Red zone		Yellow zone		Orange zone	
scenario	Model	95% IC	Reduced Chi-Sqr	95% IC	Reduced Chi-Sqr	95% IC	Reduced Chi-Sqr
Flash	Linear	75.21	307,95			169.7	1571.50
	2fi	62.01	207,34			139.62	1063.65
	Quadratic	25.45	35,26			61.16	204.12
	Linear	1.83	0,188	1.77	0,173	2.33	0.302
JET	2fi	1.55	0,135	1.17	0,075	1.37	0.105
	Quadratic	0.77	0,032	0.88	0,038	0.47	0.011
BLEVE	Linear	8.94	4,411	13.46	9,981	20.67	23.50
	2fi	8.26	3,758	12.25	8,633	18.94	19.74
	Quadratic	1.25	0,086	1.37	0,104	1.85	0.187

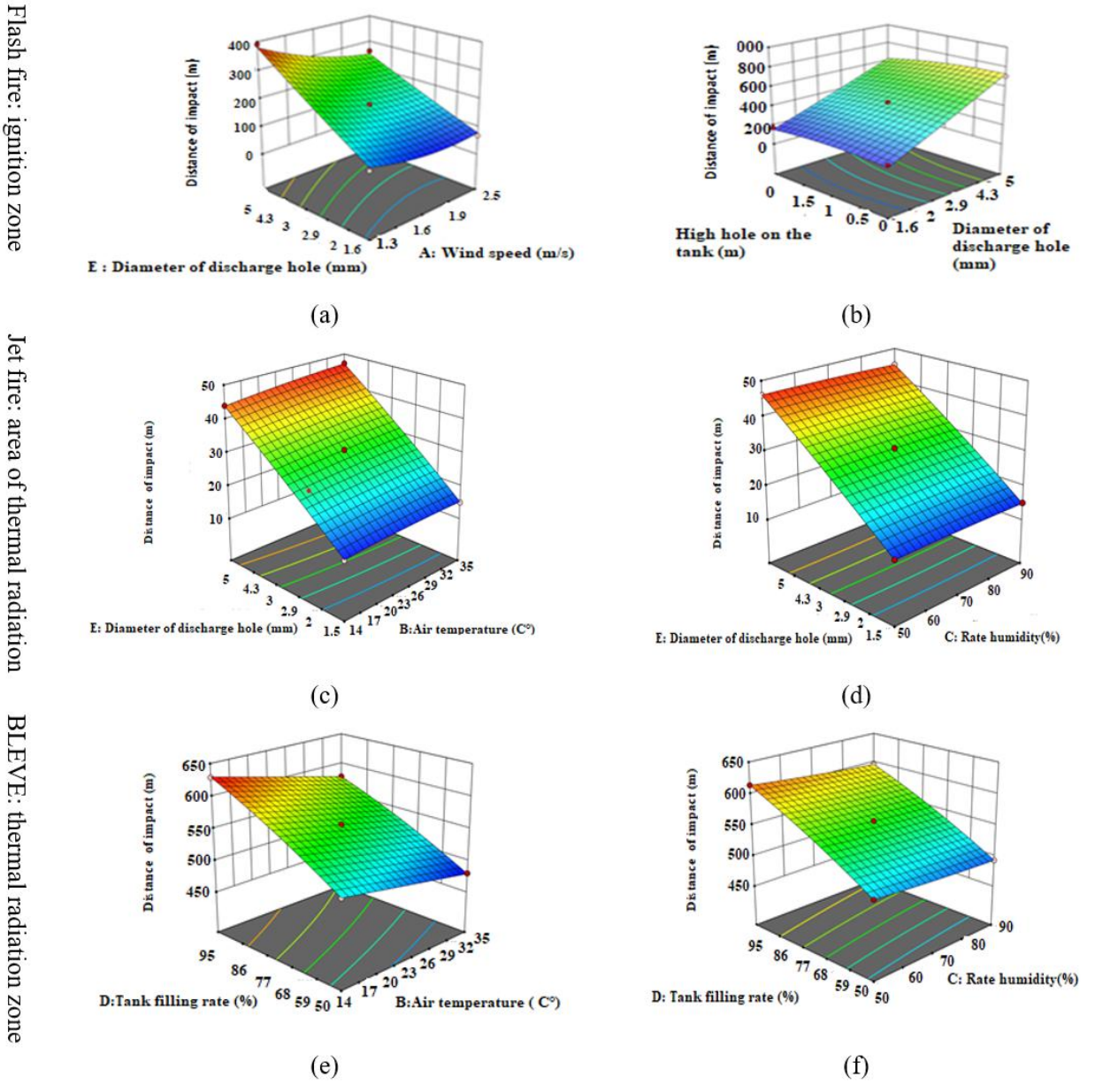

Fig. 6: Surface response of hazard zone parameter interactions. Distance impact flash fire: (a) diameter of discharge and wind speeds, (b) high hole on the tankW and diameter of discharge; distance impact Jet fire: (c) diameter of discharge and Air temperature, (d) diameter of discharge and rate humidity; distance impact BLEVE fire: (e) Tank filling rate and air temperature, (f) Tank filling rate and rate humidity.

temperature increases, the impact zone decreases because, as the air temperature rises, the difference between the fire tank temperature and the ambient temperature decreases, reducing the heat transfer surface, which in turn leads to a decreased heat-affected area.[52] The fill rate of the tank has a much higher impact compared to other parameters in a BLEVE scenario. This increase in the tank fill rate leads to an increased mass combustion rate; as the liquid disperses, it lengthens the flame, thus posing a higher thermal risk.[53] When the tank fills rate increases and the air temperature drops, the impact zone is larger. Despite the low air temperature having a negative effect on the impact zone, the combustion of the hydrocarbon mass generates a fireball that produces greater thermal radiation, which is a function of the amount of hydrocarbon contained in the tank. The combination of the tank fill rate and humidity level is presented in Fig. 6f. When the tank is almost full and the humidity level increases, a slight reduction in the hazard distance is observed. The effect of air humidity on thermal risk increases when humidity decreases.[50] Moreover, water vapor in the air influences heat exchange conditions,[51] which could likely explain this slight reduction in the thermal zone when humidity increases.

4. Conclusion

Assessing the danger zone produced by fire scenarios is a priority for the safety of people and property. The aim of this

study was to develop simplified models for hazard zone assessment. Using a Box-Behnken design of experiments, several combinations of different parameters were established, and their simulation in the ALOHA software enabled us to assess the hazard distance of different fire scenarios, most of which were divided into 3 zones (red, orange and yellow). The static analysis was used to select and analyze the different models, and the response surface revealed the interaction between the most significant parameters of the different models. The results obtained in this study reveal that the quadratic model is more suitable for the hazard zones belonging to the different fire scenarios studied; the diameter of the hydrocarbon discharge holes is the most significant parameter in the hazard zone assessment model for the flash fire and Jet scenarios, and the tank filling rate for the BLEVE scenario. The quadratic model is the most suitable for the hazard zones associated with the different fire scenarios studied. The diameter of the discharge hole and the filling rate increase with the hazard distances. In this case, tank materials and storage conditions must be known. Tank surfaces need to be protected to attenuate any shocks that may cause holes in the tank, and the filling capacity of the liquid in the tank needs to be controlled. It may be advisable for industries to increase tank inspections and constantly evaluate their emergency response plans in the event of a fire scenario. Some suggestions for future studies can be made according to results obtained here. One can use in the simulation other hazard zone simulation tools such as EFFECTS, TerEX and PHAST. Moreover modelling studies can be performed by taking into account additional parameters such as the shape of the fluid discharge diameter, the fluid's calorific value, etc. This could provide a model with more efficient results.

Acknowledgments
Special thanks to Dr. Fabien Kenmogne for his scientific support in the completion of this article and Dr Loick Kodjom Foko for data analysis.

Conflict of Interest
There is no conflict of interest.

Supporting Information
Applicable.

References
[1] R. Z. Ríos-Mercado, C. Borraz-Sánchez, Optimization problems in natural gas transportation systems: a state-of-the-art review, *Applied Energy*, 2015, **147**, 536-555, doi: 10.1016/j.apenergy.2015.03.017.
[2] A. J. Schneller, K. A. Smemo, E. Mangan, C. Munisteri, C. Hobbs, C. MacKay, Crude oil transportation by rail in Saratoga County, New York: public perceptions of technological risk, state responses, and policy, *Risk, Hazards & Crisis in Public Policy*, 2020, **11**, 377-410, doi: 10.1002/rhc3.12200.
[3] E. Erkut, S. A. Tjandra, and V. Verter, Chapter 9 Hazardous Materials Transportation, *Handbooks in Operations Research and Management Science*, 2007, **14**, 539-621, doi: 10.1016/S0927-0507(06)14009-8.
[4] A. Hart, A review of technologies for transporting heavy crude oil and bitumen *via* pipelines, *Journal of Petroleum Exploration and Production Technology*, 2014, **4**, 327-336, doi: 10.1007/s13202-013-0086-6.
[5] S. Welch, S. Youn, A. Nichols, S. Na, R. Shen, Transportation of hazardous material *via* railroad: incident investigation and a case study of derailment in 2023, *Process Safety Progress*, 2024, **43**, 570-578, doi: 10.1002/prs.12598.
[6] Y. Zhu, X. Qian, Z. Liu, P. Huang, M. Yuan, Analysis and assessment of the Qingdao crude oil vapor explosion accident: Lessons learnt, *Journal of Loss Prevention in the Process Industries*, 2015, **33**, 289-303, doi: 10.1016/j.jlp.2015.01.004.
[7] L. T. Singer, F. Schumacher, J. Fabisiak, L. J. Dietz, T. Ciesielski, The east Palestine train derailment: a complex environmental disaster, *Neurotoxicology and Teratology*, 2025, **110**, 107522, doi: 10.1016/j.ntt.2025.107522.
[8] C. Frederick, Environmental pollution control engineering, *Journal of Environmental Quality*, 1993, **22**, 214, doi: 10.2134/jeq1993.00472425002200010032x.
[9] B. Sun, K. Guo, V. K. Pareek, Computational fluid dynamics simulation of LNG pool fire radiation for hazard analysis, *Journal of Loss Prevention in the Process Industries*, 2014, **29**, 92-102, doi: 10.1016/j.jlp.2014.02.003.
[10] A. Palacios, B. Rengel, J. Casal, E. Pastor, E. Planas, Computational fluid dynamics modelling of hydrocarbon fires in open environments: Literature review, *The Canadian Journal of Chemical Engineering*, 2020, **98**, 2381-2396, doi: 10.1002/cjce.23768.
[11] G. Hankinson, B. J. Lowesmith, A consideration of methods of determining the radiative characteristics of jet fires, *Combustion and Flame*, 2012, **159**, 1165-1177, doi: 10.1016/j.combustflame.2011.09.004.
[12] J. Wang, M. Wang, X. Yu, R. Zong, S. Lu, Experimental and numerical study of the fire behavior of a tank with oil leaking and burning, *Process Safety and Environmental Protection*, 2022, **159**, 1203-1214, doi: 10.1016/j.psep.2022.01.047.
[13] H. Boot, Developments in modelling of thermal radiation from pool and jet fires, *Chemical Engineering Transactions*, 2016, **48**, 67-72, doi: 10.3303/CET1648012.
[14] N. Mišić, D. Zigar, A. Božilov, D. Pešić, Calculation of thermal radiation level during a pool fire caused by leakage of kerosene from tanker wagon at railway crossings, *TRANSACTIONS of the VŠB – Technical University of Ostrava, Safety Engineering Series*, 2018, **13**, 29-36, doi: 10.2478/tvsbses-2018-0005.
[15] A. Bernatik, W. Zimmerman, M. Pitt, M. Strizik, V. Nevrly, Z. Zelinger, Modelling accidental releases of dangerous gases into the lower troposphere from mobile sources, *Process Safety and Environmental Protection*, 2008, **86**, 198-207, doi: 10.1016/j.psep.2007.12.002.
[16] O. Hassan, Z. A. Khan, M. Irfan, M. I. Rashid, Beyond

ALOHA- quickly predict accidental release of toxic chemicals using machine learning, *Journal of Loss Prevention in the Process Industries*, 2025, **94**, 105542, doi: 10.1016/j.jlp.2024.105542.
[17] A. H. da Silva Jr, C. R. S. de Oliveira, J. Fiates, Numerical experimental design application in consequence analysis of ammonia leakage, *Chemical Engineering Journal Advances*, 2022, **11**, 100327, doi: 10.1016/j.ceja.2022.100327.
[18] D. Saloglu, H. Dertli, M. Mohammadi, M. Mohammadi, Emission rates, ALOHA simulation and Box-Behnken design of accidental releases in butyl acrylate tank - case study, *Production Engineering Archives*, 2022, **28**, 346-358, doi: 10.30657/pea.2022.28.43.
[19] F. Van den Schoor, F. Verplaetsen, The upper explosion limit of lower alkanes and alkenes in air at elevated pressures and temperatures, *Journal of Hazardous Materials*, 2006, **128**, 1-9, doi: 10.1016/j.jhazmat.2005.06.043.
[20] J. Casal Fàbrega, M. Gómez-Mares, M. Á. Muñoz, A. Palacios, Jet fires: a minor major accident, *Chemical Engineering Transactions*, 2012, **26**, 13-20, doi: 10.3303/CET1226003.
[21] P. Blankenhagel, K. D. Wehrstedt, K. B. Mishra, J. Steinbach, Thermal radiation assessment of fireballs using infrared camera, *Journal of Loss Prevention in the Process Industries*, 2018, **54**, 246-253, doi: 10.1016/j.jlp.2018.04.008.
[22] N. Bariha, I. M. Mishra, V. C. Srivastava, Fire and explosion hazard analysis during surface transport of liquefied petroleum gas (LPG): a case study of LPG truck tanker accident in Kannur, Kerala, India, *Journal of Loss Prevention in the Process Industries*, 2016, **40**, 449-460, doi: 10.1016/j.jlp.2016.01.020.
[23] H. Zhu, Z. Mao, Q. Wang, J. Sun, The influences of key factors on the consequences following the natural gas leakage from pipeline, *Procedia Engineering*, 2013, **62**, 592-601, doi: 10.1016/j.proeng.2013.08.104.
[24] A. Bernatik, W. Zimmerman, M. Pitt, M. Strizik, V. Nevrly, Z. Zelinger, Modelling accidental releases of dangerous gases into the lower troposphere from mobile sources, *Process Safety and Environmental Protection*, 2008, **86**, 198-207, doi: 10.1016/j.psep.2007.12.002.
[25] M. Kelrykh, O. Fomin, J. Gerlici, P. Prokopenko, K. Kravchenko, T. Lack, Features of tank car testing for dangerous cargoes transportation, *IOP Conference Series*: *Materials Science and Engineering*, 2019, **659**, 012055, doi: 10.1088/1757-899X/659/1/012055.
[26] A. Tchoukouabe, Z. M. Ayissi, B. Samuel, R. Mouangue, Analysis and spatiotemporal evaluation of the effects of the determinants of accidental atex fires linked to rail mobility: scenario approach, *EMERG - Energy Environment Efficiency Resources Globalization*, 2025, **11**, 57-81, doi: 10.37410//emerg.2025.1.05.
[27] S. L. C. Ferreira, R. E. Bruns, H. S. Ferreira, G. D. Matos, J. M. David, G. C. Brandão, E. G. P. da Silva, L. A. Portugal, P. S. dos Reis, A. S. Souza, W. N. L. dos Santos, Box-Behnken design: an alternative for the optimization of analytical methods, *Analytica Chimica Acta*, 2007, **597**, 179-186, doi: 10.1016/j.aca.2007.07.011.
[28] K. D. Tocher, The design and analysis of block experiments, *Journal of the Royal Statistical Society Series B*: *Statistical Methodology*, 1952, **14**, 45-91, doi: 10.1111/j.2517-6161.1952.tb00101.x.
[29] S. N. Nam, H. Cho, J. Han, N. Her, J. Yoon, Photocatalytic degradation of acesulfame K: optimization using the box–behnken design (BBD), *Process Safety and Environmental Protection*, 2018, **113**, 10-21, doi: 10.1016/j.psep.2017.09.002.
[30] S. L. C. Ferreira, R. E. Bruns, H. S. Ferreira, G. D. Matos, J. M. David, G. C. Brandão, E. G. P. da Silva, L. A. Portugal, P. S. dos Reis, A. S. Souza, W. N. L. dos Santos, Box-Behnken design: an alternative for the optimization of analytical methods, *Analytica Chimica Acta*, 2007, **597**, 179-186, doi: 10.1016/j.aca.2007.07.011.
[31] F. Bernardeau, Skewness and kurtosis in large-scale cosmic fields, *The Astrophysical Journal*, 1994, **433**, 32, doi: 10.1086/174620.
[32] S. DemİR, Comparison of normality tests in terms of sample sizes under different skewness and kurtosis coefficients, *International Journal of Assessment Tools in Education*, 2022, **9**, 397-409, doi: 10.21449/ijate.1101295.
[33] G. Hatem, J. Zeidan, M. Goossens, C. Moreira, Normality testing methods and the importance of skewness and kurtosis in statistical analysis, *BAU Journal - Science and Technology*, 2022, **3**, 1-7, doi: 10.54729/ktpe9512
[34] L. J. Saunders, R. A. Russell, D. P. Crabb, The coefficient of determination: what determines a useful R^2 statistic? *Investigative Opthalmology & Visual Science*, 2012, **53**, 6830, doi: 10.1167/iovs.12-10598.
[35] L. St›hle, S. Wold, Analysis of variance (ANOVA), *Chemometrics and Intelligent Laboratory Systems*, 1989, **6**, 259-272, doi: 10.1016/0169-7439(89)80095-4.
[36] P. A. Castillo, M. G. Arenas, N. Rico, A. M. Mora, P. García-Sánchez, J. L. J. Laredo, J. J. Merelo, Determining the significance and relative importance of parameters of a simulated quenching algorithm using statistical tools, *Applied Intelligence*, 2012, **37**, 239-254, doi: 10.1007/s10489-011-0324-x.
[37] S. Menard, Coefficients of determination for multiple logistic regression analysis, *The American Statistician*, 2000, **54**, 17-24, doi: 10.1080/00031305.2000.10474502.
[38] J. Ji, J. Xu, Y. Xiao, Y. Luan, Evaluation of improved model to accurately monitor soil water content, *Water*, 2021, **13**, 3441, doi: 10.3390/w13233441.
[39] K. D. Young, R. J. Lewis, What is confidence? part 1: the use and interpretation of confidence intervals, *Annals of Emergency Medicine*, 1997, **30**, 307-310, doi: 10.1016/S0196-0644(97)70166-5.
[40] B. Shipley, The AIC model selection method applied to path analytic models compared using a d-separation test, *Ecology*, 2013, **94**, 560-564, doi: 10.1890/12-0976.1.
[41] R. C. MacCallum, C. M. Mar, Distinguishing between moderator and quadratic effects in multiple regression, *Psychological Bulletin*, 1995, **118**, 405-421, doi: 10.1037/0033-2909.118.3.405.
[42] F. Valiyan, H. Koohsari, A. Fadavi, Use of Response surface

methodology to investigate the effect of several fermentation conditions on the antibacterial activity of several kombucha beverages, *Journal of Food Science and Technology*, 2021, **58**, 1877-1891, doi: 10.1007/s13197-020-04699-6.
[43] J. B. Gray, W. H. Woodall, The maximum size of standardized and internally studentized residuals in regression analysis, *The American Statistician*, 1994, **48**, 111-113, doi: 10.1080/00031305.1994.10476035.
[44] R. Ospina, F. Marmolejo-Ramos, Performance of some estimators of relative variability, *Frontiers in Applied Mathematics and Statistics*, 2019, **5**, 43, doi: 10.3389/fams.2019.00043.
[45] S. H. Tan, S. B. Tan, The correct interpretation of confidence intervals, *Proceedings of Singapore Healthcare*, 2010, **19**, 276-278, doi: 10.1177/201010581001900316.
[46] R. Wirangga, D. Mugisidi, A. T. Sayuti, O. Heriyani, The impact of wind speed on the rate of water evaporation in a desalination chamber, *Journal of Advanced Research in Fluid Mechanics and Thermal Sciences*, 2023, **106**, 39-50, doi: 10.37934/arfmts.106.1.3950.
[47] H. Davarzani, K. Smits, R. M. Tolene, T. Illangasekare, Study of the effect of wind speed on evaporation from soil through integrated modeling of the atmospheric boundary layer and shallow subsurface, *Water Resources Research*, 2014, **50**, 661-680, doi: 10.1002/2013WR013952.
[48] R. Bubbico, B. Mazzarotta, Accidental release of toxic chemicals: influence of the main input parameters on consequence calculation, *Journal of Hazardous Materials*, 2008, **151**, 394-406, doi: 10.1016/j.jhazmat.2007.06.002.
[49] Q. Xie, L. Xiang, J. Zhang, Q. Lu, F. Zhou, Mutual effects between dynamic leakage behavior and the pressure/temperature in a LNG tank with external heat fluxes, *Journal of Loss Prevention in the Process Industries*, 2020, **63**, 104029, doi: 10.1016/j.jlp.2019.104029.
[50] X. Chen, N. Li, J. Liu, Z. Zhang, Y. Liu, Global heat wave hazard considering humidity effects during the 21st century, *International Journal of Environmental Research and Public Health*, 2019, **16**, 1513, doi: 10.3390/ijerph16091513.
[51] A. Sobolewski, M. Młynarczyk, M. Konarska, J. Bugajska, The influence of air humidity on human heat stress in a hot environment, *International Journal of Occupational Safety and Ergonomics*, 2021, **27**, 226-236, doi: 10.1080/10803548.2019.1699728.
[52] H. Ranjan, A. K. Bharti, M. S. Emani, J. P. Meyer, S. K. Saha, New combined heat transfer enhancement techniques used in laminar flow through non-circular ducts, *Applied Thermal Engineering*, 2019, **163**, 114325, doi: 10.1016/j.applthermaleng.2019.114325.
[53] J. Wang, X. Chen, Y. Li, M. Wang, X. Yu, R. Zong, S. Lu, Effects of filling level and tray size on the burning behavior of a tank during burning of leaking contents: an integrated experimental and numerical approach, *Process Safety and Environmental Protection*, 2022, **168**, 513-525, doi: 10.1016/j.psep.2022.10.018.

Publisher's Note: Engineered Science Publisher remains neutral with regard to jurisdictional claims in published maps and institutional affiliations.

Open Access

This article is licensed under a Creative Commons Attribution 4.0 International License, which permits the use, sharing, adaptation, distribution and reproduction in any medium or format, as long as appropriate credit to the original author(s) and the source is given by providing a link to the Creative Commons license and changes need to be indicated if there are any. The images or other third-party material in this article are included in the article's Creative Commons license, unless indicated otherwise in a credit line to the material. If material is not included in the article's Creative Commons license and your intended use is not permitted by statutory regulation or exceeds the permitted use, you will need to obtain permission directly from the copyright holder. To view a copy of this license, visit http://creativecommons.org/ licenses/by/4.0/.

©The Author(s) 2025